ACS Catalysis

pubs.acs.org/acscatalysis Research Article

Iron-Carbene Initiated O−H Insertion/Aldol Cascade for the Stereoselective Synthesis of Functionalized Tetrahydrofurans

Prakash Kafle, Bidhan Ghosh,‡ Arianne C. Hunter,‡ Rishav Mukherjee,‡ Kenneth M. Nicholas, and Indrajeet Sharma*

Cite This: ACS Catal. 2024, 14, 1292−1299 Read Online

ACCESS | Metrics & More | Article Recommendations | Supporting Information

ABSTRACT: Given its earth abundance, cost-effectiveness, and ecofriendly qualities, iron serves as a promising alternative to precious metals in catalysis. This article presents an iron carbene-initiated cascade approach for synthesizing highly substituted tetrahydrofurans at the gram scale. This cascade reaction utilizes readily accessible β-hydroxyketones and diazo compounds and works with iron catalyst loading as low as 5 mol %. This reaction proceeds through an O−H insertion into diazo-derived iron carbenes, followed by an intramolecular aldol reaction to access functionalized tetrahydrofurans in high yields and diastereoselectivity. The versatile nature of this domino sequence accommodates diverse β-hydroxyketones and diazo compounds, streamlining access to synthetically challenging spiroethers. Furthermore, this cascade process offers a route to enantiopure tetrahydrofurans by utilizing a diazo ester bearing a chiral auxiliary, 8-phenylmenthol. Postmodifications of the tetrahydrofuran product provide access to various analogues, including a medicinally relevant oxetane motif. Density functional theory (DFT) calculations substantiate a stereospecific mechanism wherein the intramolecular aldol reaction proceeds via a fused six- and five-membered iron−oxygen transition-state complex, yielding the contrathermodynamic *cis*-aldol product.

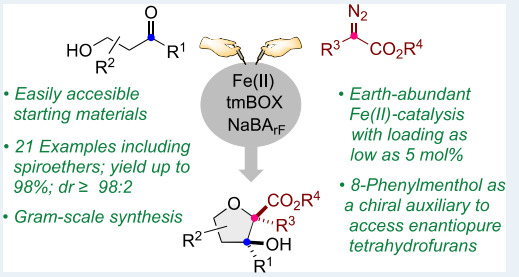

KEYWORDS: *iron catalysis, cascade reactions, diazo compounds, tetrahydrofurans, chiral auxiliary*

Metal catalysts play a pivotal role in synthetic chemistry. Iron (Fe) stands out as the second most abundant metal in the Earth's crust, following only aluminum, with a composition of approximately 4.7% by weight.[1] This abundance, combined with iron's low cost and relative nontoxic nature, positions it as the catalyst of choice for various chemical transformations.[2] Incorporating iron catalysts into synthetic processes can reduce the cost of producing pharmaceuticals, fertilizers, and other essential products, as the expense of reagents directly influences compound cost. Furthermore, iron boasts a commendable safety profile endorsed by regulatory authorities. It is considered "a metal with a minimal safety concern", as 1300 ppm residual iron is deemed acceptable in drug substances. This status represents a distinct advantage compared to the ≤10 ppm prescribed for most other transition metals, including rhodium.[1b] These characteristics elevate iron as a sustainable catalyst for chemical synthesis, presenting economic benefits and enhanced safety features.[2,3] Another crucial factor contributing to cost-effective chemical synthesis involves adopting cascade reactions, which have garnered substantial research interest in recent years.[4] These reactions offer remarkable advantages, encompassing atom economy, a substantial saving in time, labor, resources, and waste management.[5] Cascade reactions introduce notable efficiencies by consolidating multiple transformations within a singular synthetic process. For example, a product traditionally requiring several sequential steps can now be obtained through a singular reaction solvent, workup procedure, and purification phase. In this context, our research group[6] and numerous others have pioneered cascade reactions utilizing diazo-derived rhodium carbenes.[7]

Rhodium is one of the most utilized metals in diazo chemistry.[8] However, due to its high cost and limited availability, we have shifted our focus toward developing cascade reactions utilizing environmentally sustainable, earth-abundant metal catalysts, including iron, copper, and zinc.[9] Despite the decades-long recognition of iron carbene complexes, the utilization of iron in carbene cascade reactions has remained unexplored, likely due to the challenge of identifying an iron catalyst complex that effectively stabilizes the necessary zwitterionic intermediate required to trigger a cascade reaction.[10] To the best of our knowledge, there is no report of a cascade reaction involving diazo-derived iron carbenes. However, multiple research groups have reported N−H, O−H, S−H, and Si−H bond insertion reactions,[11]

Received: October 21, 2023
Revised: December 22, 2023
Accepted: December 26, 2023
Published: January 10, 2024

https://doi.org/10.1021/acscatal.3c05040
ACS Catal. 2024, 14, 1292−1299

cyclopropanations,[12] and C−H functionalization reactions of iron carbenes.[13] We conceived of employing iron as a catalyst within the established carbene-initiated O−H-insertion/aldol cascade as a starting point. This methodology aims to enable access to functionalized tetrahydrofurans, commonly found in naturally occurring bioactive substances spanning diverse classes such as lignans, acetogenins, ionophores, and macrolides.[14] Notable examples include (+)-fragransin A2,[15] caloxylane,[16] and amphidinolide F[17] (Figure 1).

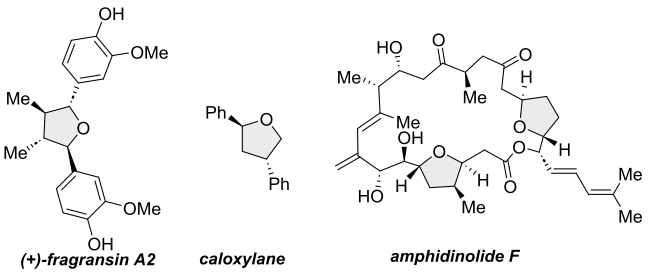

Figure 1. Naturally occurring tetrahydrofurans.

Multiple strategies have been developed to attain the stereoselective synthesis of tetrahydrofurans.[18] Despite significant progress in synthetic methodologies, synthesizing substituted tetrahydrofurans remains formidable, underscoring the need to explore innovative approaches. The Moody and the Hu group reported rhodium(II)-catalyzed reactions of diazocarbonyl compounds with β-hydroxyketones to access highly substituted tetrahydrofurans (Figure 2a).[19] Our group

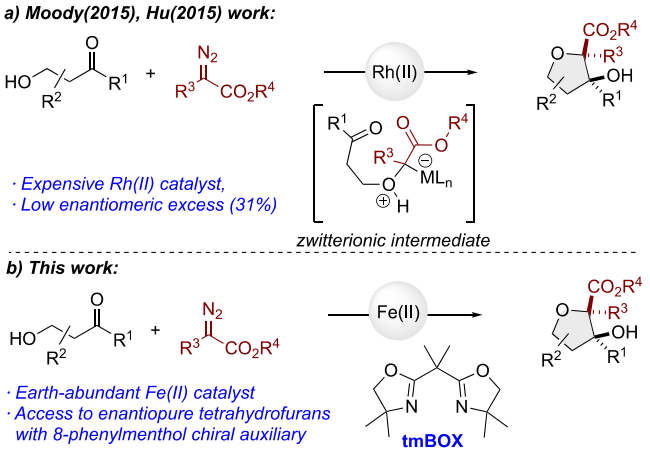

Figure 2. (a) Previously known rhodium-catalyzed approaches. (b) This work: iron catalyzed carbene cascade.

developed a cascade reaction involving O−H insertion/aldol/oxy-Cope sequence to access medium-sized rings.[6b] Taking inspiration from these studies, we introduce an inexpensive iron catalyst in diazocarbene chemistry to synthesize highly substituted tetrahydrofurans (Figure 2b).

Taking inspiration from the Zhou group,[11a] we envisioned that BOX ligand would coordinate and stabilize the Fe(II) catalyst. At the same time, sodium tetrakis(3,5-bis-(trifluoromethyl)phenyl)borate ($NaBAr_F$) would initiate a counterion exchange to create a highly Lewis acidic Fe(II) complex that would effectively decompose the diazo. Therefore, we initiated our optimization studies for the iron-catalyzed cascade reaction with readily available starting materials keto-alcohol **1a**, and diazo **2a** as model substrates to access the desired tetrahydrofurans (Table 1).

Table 1. Optimization of the Reaction Conditions[a]

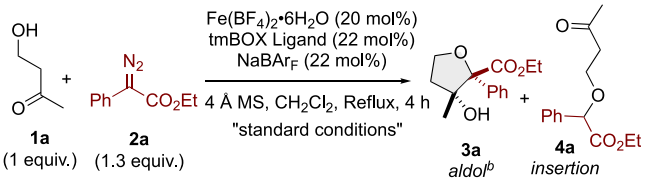

entry	variation from "standard conditions"	% yield[c]	3a/4a[d]
1	none	95%	8:1
2[e]	low catalyst loading (5 mol %)	83%	8:1
3	no 4 Å MS	70%	6:1
4	$FeCl_3$ instead of $Fe(BF_4)_2$•$6H_2O$	50%	3:1
5	$FeCl_2$ instead of $Fe(BF_4)_2$•$6H_2O$	n.r.	n.d.
6	no $Fe(BF_4)_2$•$6H_2O$	n.r.	n.d.
7	no tmBOX	70%	1:1
8	no $NaBAr_F$	75%	1:3
9	44 mol % of $NaBAr_F$	80%	1:2.5
10	44 mol % of tmBOX	20%	1:1
11	$CHCl_3$ as solvent	70%	1:1
12	DCE as solvent	60%	4:1
13	no syringe pump addition	40%	1:1

[a]All reactions were performed by adding diazo compound **2a** (1.3 equiv, 0.15 M CH_2Cl_2) dropwise via syringe pump to a solution of keto-alcohol **1a** (1.0 equiv), $Fe(BF_4)_2$•$6H_2O$ (20 mol %), $NaBAr_F$ (22 mol %), and tmBOX (22 mol %) in 0.2 M CH_2Cl_2. [b]Diastereomeric ratio (dr) of **3a** was determined by ^{1}H NMR (dr ≥ 98:2). [c]Yield was determined by ^{1}H NMR using 1,3,5-trimethoxybenzene as an internal standard. [d]Selectivity (**3a**/**4a**) was determined by ^{1}H NMR. [e]$Fe(BF_4)_2$•$6H_2O$ (5 mol %), $NaBAr_F$ (5.5 mol %), and tmBOX (5.5 mol %) was used. n.r. = no reaction; n.d. = not determined.

Following a thorough evaluation of various reaction conditions, we discovered that the optimal results, with a yield of 95% and an aldol/insertion ratio of 8:1, could be obtained by using $Fe(BF_4)_2$•$6H_2O$ (20 mol %), tetramethyl-bis(oxazoline) (tmBOX) (22 mol %) and $NaBAr_F$ (22 mol %) in methylene chloride with 4 Å molecular sieves. The reaction was carried out by adding a solution of diazo compound **2a** in methylene chloride to the reaction mixture under reflux conditions using a syringe pump for 1.5 h (entry 1). The ^{1}H NMR analysis confirmed the formation of a single diastereomer (dr ≥ 98:2) of the aldol product. Subsequently, we evaluated the reaction's effectiveness using a low (5 mol %) catalyst loading and were delighted to find a similar outcome as with 20 mol % loading (entry 2). It is noteworthy to mention that we use 20 mol % of iron catalyst in our standard conditions as it is more practical to weigh. Significantly, the absence of 4 Å molecular sieves reduced both the yield and the aldol/insertion ratio (entry 3). $FeCl_3$ also catalyzed the aldol reaction but resulted in low yield and selectivity (entry 4). Conversely, $FeCl_2$ was observed to be unreactive in this context (entry 5). Without $Fe(BF_4)_2$•$6H_2O$, no desired product was obtained (entry 6). Without the tmBox, the reaction provided a good yield but a lower aldol/insertion ratio for the desired product (entry 7). Likewise, in the absence of $NaBAr_F$, the reaction proceeded with a comparable yield but exhibited an increase in the insertion product (entry 8). Particularly, $NaBAr_F$ has been shown to enhance the Lewis

https://doi.org/10.1021/acscatal.3c05040
ACS Catal. 2024, 14, 1292−1299

acidity and electrophilicity of the iron catalyst by exchanging the counteranion with a bulky and noncoordinating BAr_F anion, resulting in improvements in reaction efficiencies[13b,20] and consequently improving the aldol/insertion ratio. However, augmenting the quantity of $NaBAr_F$ (2 equiv) results in the rapid decomposition of the diazo compound, leading to a faster reaction with an increased amount of the insertion product (entry 9). Additionally, increasing the loading of the tmBox ligand reduced iron's catalytic activity, thereby decreasing the yield, and a lower aldol/insertion ratio was observed (entry 10). Subsequently, our efforts were directed toward optimizing the solvent for this reaction. Chloroform and 1,2-dichloroethane (DCE) demonstrated solvent compatibility, although the yield and aldol/insertion ratio were reduced. Despite this, none of these solvents outperformed dichloromethane, leading to its selection for further investigations (entries 11, 12). We eventually discovered that the slow addition of the diazo compound using a syringe pump over 1.5 h is crucial in achieving the desired yield and a high aldol selectivity (entry 13).

After establishing the optimal conditions, we investigated the scope of α-aryl-α-diazocarbonyl compounds, also known as donor−acceptor diazos[21] (Table 2). At first, substituting the ester group of the diazo compound from ethyl to methyl ester resulted in the formation of the corresponding product **3b** with a comparable yield, and a similar aldol:insertion ratio (10:1) was obtained. Next, we focused on examining different electronic substituents in the aryl group. Notably, electron-donating groups such as methyl and methoxy at the para-position of the phenyl ring provided excellent yields of the desired products (**3c**, **3d**) with favorable aldol/insertion ratios. Similarly, the electron-donating thiophene diazo afforded the corresponding product **3e** in excellent yield with 1:1 aldol/insertion selectivity. Conversely, the electron-withdrawing nitro substituent afforded a lower yield (35%) of desired product **3f** with 4:1 aldol/insertion selectivity.

Moreover, when a halogen was substituted at the *para* position of the phenyl group, the transformation smoothly proceeded to afford the desired product with an outstanding yield (**3g**). Notably, the cyclic diazo compounds proceeded in high yield to provide the desired spiroethers (**3h**), which are challenging to obtain with high stereoselectivity. Diazo compounds derived from tetralone also provided the desired spiroethers in good yield (**3i**).

Next, we aimed to explore the range of substrates for different hydroxyketones (Table 3). We introduced various keto-substituted groups to evaluate their compatibility with diazo substrate **2**. Keto-alcohols **1**, containing substituents such as phenyl, *p*-Me-phenyl, and *p*-Br-phenyl, all underwent smooth reactions with diazo **2** and resulted in the formation of the desired products **3j**−**l**, with yields ranging from 50 to

Table 2. Scope of Diazo Compounds[a]

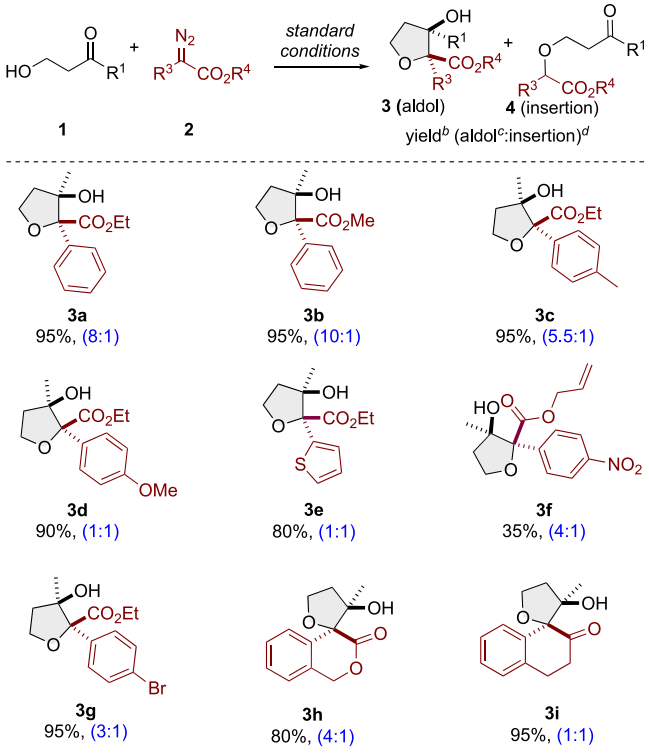

[a]All reactions were performed by adding diazo compound **2** (1.3 equiv, 0.15 M CH_2Cl_2) dropwise via a syringe pump to a solution of keto-alcohol **1** (1.0 equiv), $Fe(BF_4)_2{\bullet}6H_2O$ (20 mol %), $NaBAr_F$ (22 mol %), and tmBOX (22 mol %) in 0.2 M CH_2Cl_2. [b]Yield was determined by ^1H NMR using 1,3,5-trimethoxybenzene as an internal standard. [c]Diastereomeric ratio was determined by ^1H NMR (dr ≥ 98:2). [d]Selectivity was determined by ^1H NMR.

Table 3. Scope of β-Hydroxyketones[a]

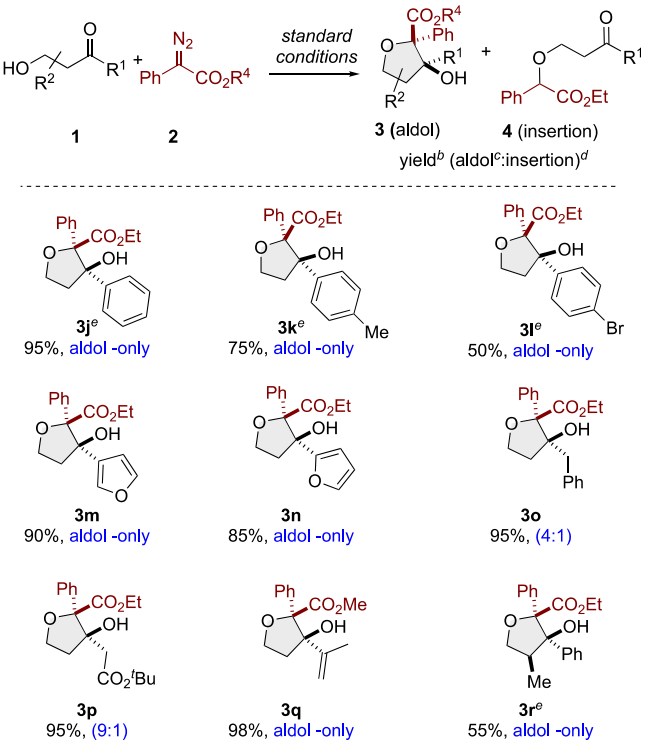

[a]All reactions were performed by adding diazo compound **2** (1.3 equiv, 0.15 M CH_2Cl_2) dropwise via syringe pump to a solution of keto-alcohol **1** (1.0 equiv), $Fe(BF_4)_2{\bullet}6H_2O$ (20 mol %), $NaBAr_F$ (22 mol %), and tmBOX (22 mol %) in 0.2 M CH_2Cl_2. [b]Yield was determined by ^1H NMR using 1,3,5-trimethoxybenzene as an internal standard. [c]Diastereomeric ratio was determined by ^1H NMR (dr ≥ 98:2). [d]Selectivity was determined by ^1H NMR. [e]Diazo compound **2** (1.3 equiv, 0.15 M CH_2Cl_2) dropwise via syringe pump to a solution of keto-alcohol **1** (1.0 equiv), $Fe(BF_4)_2{\bullet}6H_2O$ (30 mol %), $NaBAr_F$ (32 mol %), and tmBOX (32 mol %) in 0.2 M CH_2Cl_2.

https://doi.org/10.1021/acscatal.3c05040
ACS Catal. 2024, 14, 1292−1299

95%. Furthermore, 2- and 3-substituted furan containing hydroxyketones afforded the corresponding tetrahydrofurans with a high yield and exclusive aldol selectivity (**3m**−**n**). It is important to note that the presence of the α,β-unsaturated carbonyl functionality yielded only the aldol product exclusively in every case. Surprisingly, we did not observe any insertion products with these substrates. Ketones bearing acidic α-hydrogens were well tolerated and furnished the corresponding products (**3o**, **p**) with an excellent yield (95%) and a high aldol-selectivity. Pleasantly, substituted vinyl keto-alcohol displayed efficient reactivity, forming the corresponding product **3q** in an excellent yield of 98% and with exclusive formation of the aldol product. Encouragingly, a 2-methyl-substituted keto-alcohol yielded the related aldol product **3r** exclusively, albeit with a moderate yield (55%). Importantly, the methyl and the hydroxyl groups were found to be in the *cis* conformation. This is presumably due to steric interaction arising from the α-methyl and phenyl groups of the β-hydroxyketone in the 5-6-membered fused transition state (see SI page S15 for details).

The stereochemistry of the aldol product was unequivocally established by the single crystal X-ray analysis of compounds **3h** (CCDC 2285941) and **3q** (CCDC 2285940) (Figure 3).[22]

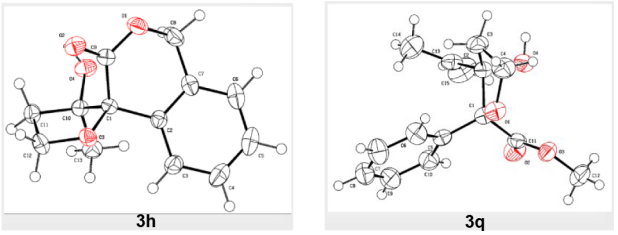

Figure 3. Single crystal X-ray structures of tetrahydrofuran **3h** and **3q**.

Significantly, the newly formed stereocenters in the aldol product have the hydroxyl and ester groups on the same side. This observation suggests a well-organized transition state during the formation of the aldol product.

Next, we focused on synthesizing enantiopure tetrahydrofurans by using chiral ligands on iron. Initially, we employed various chiral BOX-ligands (**L1**−**L3**) to induce enantiomeric excess (ee), as shown in Figure 4a. Although tetrahydrofuran **3a** was obtained in a good yield in all cases, no significant amount of ee was observed. To overcome this challenge, we devised a strategy involving an easily accessible chiral auxiliary that could be conveniently attached through the ester moiety of the diazo compound (Figure 4b).

Consequently, we synthesized esters containing chiral menthol-based auxiliaries **2s** and **2t**. The reaction of hydroxyketone **1a** with L-(−)-menthol diazo **2s** resulted in an aldol-insertion product **3s** with a 15:1 ratio in 84% yield. However, only a 2:1 diastereomeric excess (de) was observed. Significantly, when we employed the bulkier (−)-8-phenylmenthol as the chiral auxiliary, the desired diastereomeric excess was achieved in a 7:1 ratio (**3t**). To our delight, both diastereomers were easy to separate by silica gel flash column chromatography. As expected, the newly formed stereocenters in the major diastereomer had the hydroxyl and ester groups in syn fashion and had an opposite configuration to the alcohol stereocenter of 8-phenylmenthol (see the SI, page S18 for plausible transition states). The absolute stereochemistry of the predominant diastereomer **3t** was established by analyzing its

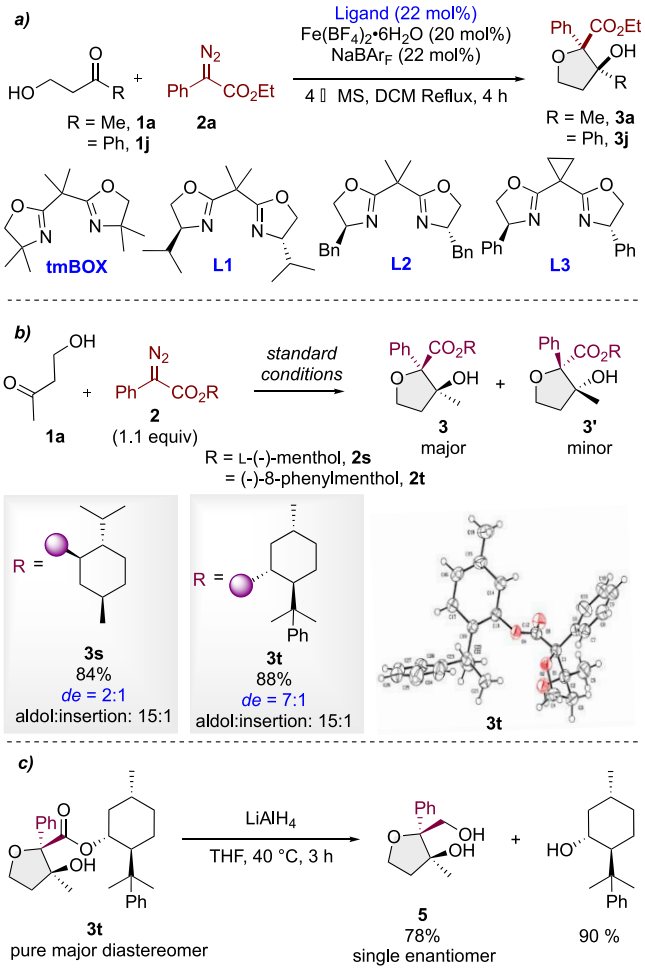

Figure 4. (a) Screening of chiral BOX-ligands. (b) Induction of diastereomeric excess (de) by a chiral auxiliary. (c) Recovery of chiral auxiliary.

crystal structure (CCDC 2285942).[22] Ultimately, the chiral auxiliary, 8-phenylmenthol, could be effectively recovered from the product through $LiAlH_4$ reduction, yielding a 90% recovery with the formation of the pure enantiomer of tetrahydrofuran **5** in 78% yield (Figure 4c).

To demonstrate the practical utility of this approach, the reaction was executed on a 4 mmol scale of β-hydroxyketone **1b**. The reaction involving diazo compound **2u** exhibited efficient progress with a notably lowered iron catalyst loading (5 mol %), affording an 80% yield (1.4 g) of the resulting **3u** compound, as illustrated in Scheme 1.

Additionally, the robustness of this method was demonstrated by successfully applying it to late-stage modifications. The ester moiety of the product was effectively converted to the corresponding alcohol **5u** through diisobutylaluminum hydride (DIBAL-H) reduction. Subsequently, compound **5u** underwent Sonogashira coupling with trimethylsilyl acetylene, forming alkyne **6** in 85% yield. A Sonogashira coupling of **5u** with phenylacetylene afforded alkyne **7** in 60% yield. Treatment of compound **7** with Mitsunobu reaction conditions furnished a dioxabicycloheptane compound **8** bearing an oxetane, which is an important motif in medicinal chemistry due to its physiochemical properties.[23] Additionally, it is important to note that the alkyne functionalities can be further

https://doi.org/10.1021/acscatal.3c05040
ACS Catal. 2024, 14, 1292−1299

Scheme 1. Gram-Scale Synthesis and Post-Modifications

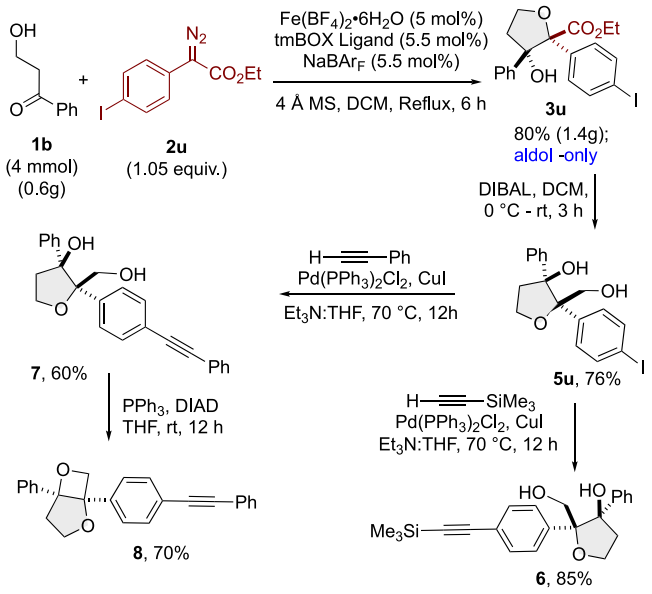

diversified using Click Chemistry to form triazoles found in various bioactive compounds and drug molecules.[24]

To gain further insights into the reaction mechanism, we synthesized the pure insertion product **4a**, following the literature-reported rhodium(II) catalyzed activation protocol, and subjected it to our optimized reaction conditions. However, the reaction did not proceed to yield the corresponding aldol product. DFT calculations also support this observation, as the insertion product **4a** is 8 kcal/mol more stable than the aldol product **3a** (Scheme 2). This experiment suggests the involvement of a metal species in the formation of an *O*-enolate intermediate, which is crucial for the subsequent progression of the aldol step.

Scheme 2. Control Experiment

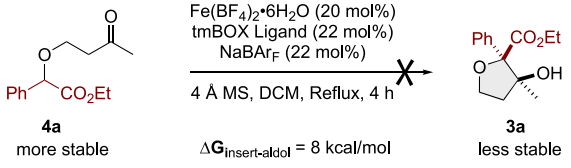

We also performed detailed density functional theory (DFT) calculations using B3LYP//6-31G(d)/LANL2DZ//vac[25] to elucidate the underlying mechanism, as shown in Figure 5.

To economize, the tmBOX ligand was replaced with an electronically similar Me_2-diimine ligand. A combination of $Fe(BF_4)_2$•$6H_2O$, Me_2-diimine, and keto alcohol is expected to produce iron carbene keto-alcohol complex **A** with extrusion of nitrogen. Intermediate **A** can engage in exergonic O−C bond formation with the bound keto alcohol to provide iron η^2-*C*-enolate **B** with the loss of the alcohol (O−H) proton. Alternatively, **B** can undergo exergonic *C*-protonation, leading to the *O*-insertion intermediate **D**. Substrate-assisted decomplexation of **D** provides the thermodynamically favored *O*-insertion product **H**. The η^2-*C*-enolate **B** is in equilibrium with the *O,O,O*-bound iron *O*-enolate **C**, favoring the latter by 7.5 kcal/mol. The *O*-enolate **C** can undergo aldol reaction via a chair-type transition state **E** (ΔG^* = 15.0 kcal/mol) to form the *cis*-iron aldol adduct **F**. Finally, proto-demetalation of **F**

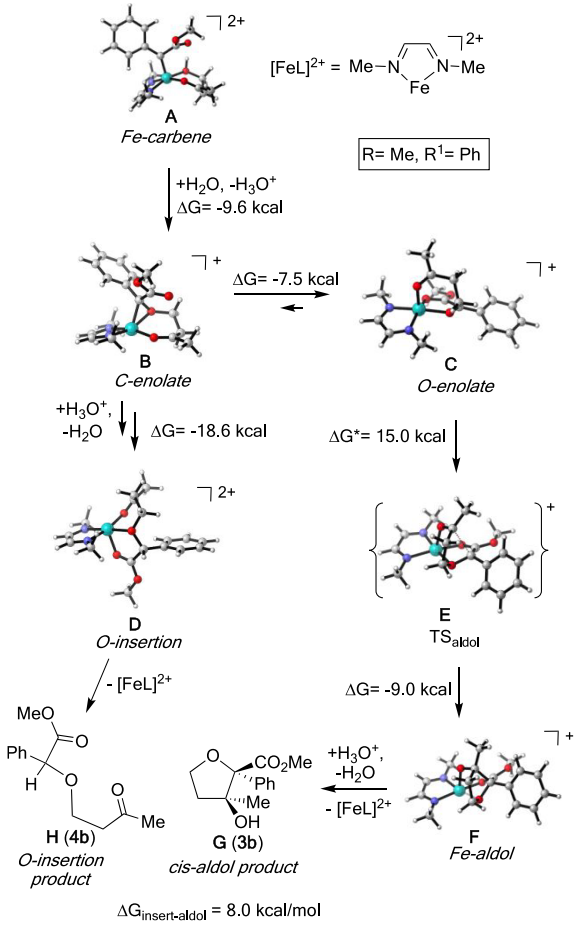

Figure 5. Computational study of the reaction mechanism (B3LYP/6-31G(d)/LANL2DZ/vac).

provides the *cis*-aldol product **G**. The iron *O,O,O*-coordination of **C**, **E**, and **F** strongly favors the experimentally observed *cis*-(OH, CO_2Et) aldol product **G**, despite being nearly isoenergetic with the *trans*-isomer (ΔG = 0.3 kcal/mol). The origin of the interesting R^1-carbonyl group effect on insertion/aldol chemoselectivity (Table 3) is not apparent from our calculations, but it could originate from a high barrier step in the proton transfer **B** to **D** insertion pathway.

Based on the literature precedent,[19a] experimental results, control experiments, and DFT studies, we propose a plausible mechanism for the iron-catalyzed O−H insertion/aldol cascade reaction, depicted in Figure 6.

The initial step involves chelating the tmBOX ligand with $Fe(BF_4)_2$•$6H_2O$ in the presence of $NaBAr_F$, forming iron-tmBOX complex **A**. Subsequently, hydroxyketone **1** coordinates with complex **A**, yielding iron-complex **B**. Next, diazoester **2** reacts with iron-complex **B**, leading to the creation of the iron-carbene intermediate **C**. Following this, insertion of an O−H transpires, generating the zwitterionic intermediate **D**, which may exist in equilibrium with an enol form **E**. Subsequently, intermediate **E** undergoes an intramolecular aldol reaction via a fused five-six-membered chair-type transition state, generating intermediate **F**. This intermediate then experiences protodemetalation, ultimately giving rise to observed tetrahydrofuran product **3** in a *cis*-diastereoselective fashion. It is essential to highlight that intermediate **D** also has the potential to undergo a [1,2]-*H* shift, resulting in the formation of the O−H insertion product **4**. This mechanism is

https://doi.org/10.1021/acscatal.3c05040
ACS Catal. 2024, 14, 1292−1299

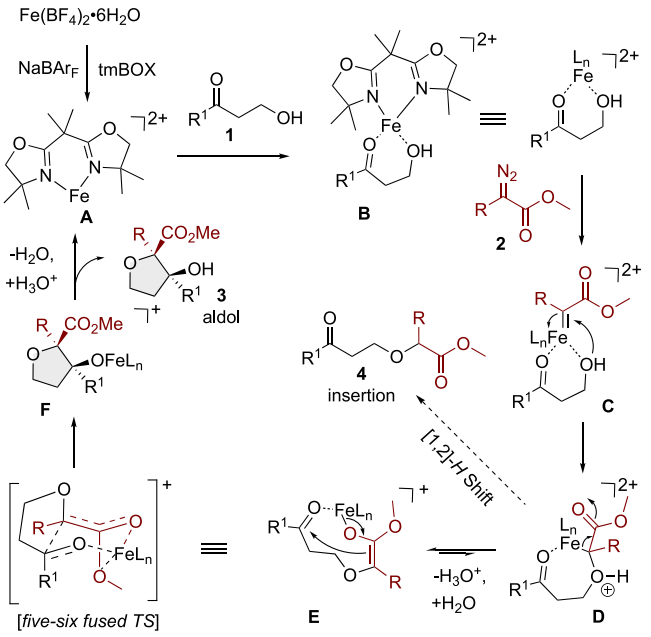

Figure 6. Plausible mechanism.

consistent with the DFT calculations and experimental findings that chiral BOX-ligands in the more stable *O*-enolate form (**E**), are not able to induce enatioinduction in the aldol step due to being far away from the reactive center, as described in the literature.[19a]

In conclusion, we devised a strategy to achieve stereoselective synthesis of highly substituted tetrahydrofurans using an O−H insertion/aldol cascade reaction. This method employs an Earth-abundant iron(II) catalyst and demonstrates tolerance toward a broad range of β-hydroxyketones and diazo compounds. The attainment of enantioselectivity in the reaction is attributed to the utilization of 8-phenylmenthol as a chiral auxiliary. The observed high stereoselectivities in the formation of tetrahydrofurans can be rationalized by proposing a mechanistic pathway supported by DFT calculations involving a fused five-six-membered transition state for the intramolecular aldol reaction. The pragmatic utility of our method has been sustained through a gram-scale synthesis of functionalized tetrahydrofurans, followed by subsequent post-modifications, including the creation of the medicinally relevant oxetane motif. Moreover, understanding iron's role as a catalyst in carbene cascade reactions will undoubtedly pave the way for novel synthetic transformations.

■ ASSOCIATED CONTENT

Supporting Information

The Supporting Information is available free of charge at https://pubs.acs.org/doi/10.1021/acscatal.3c05040.

Experimental procedures, NMR spectroscopy, and analytical data for all compounds (PDF)

Crystal coordinates information (XYZ)

■ AUTHOR INFORMATION

Corresponding Author

Indrajeet Sharma − *Department of Chemistry and Biochemistry, University of Oklahoma, Norman, Oklahoma 73019-5251, United States;* orcid.org/0000-0002-0707-0621; Email: isharma@ou.edu

Authors

Prakash Kafle − *Department of Chemistry and Biochemistry, University of Oklahoma, Norman, Oklahoma 73019-5251, United States*

Bidhan Ghosh − *Department of Chemistry and Biochemistry, University of Oklahoma, Norman, Oklahoma 73019-5251, United States*

Arianne C. Hunter − *Department of Chemistry and Biochemistry, University of Oklahoma, Norman, Oklahoma 73019-5251, United States;* orcid.org/0000-0003-1873-9682

Rishav Mukherjee − *Department of Chemistry and Biochemistry, University of Oklahoma, Norman, Oklahoma 73019-5251, United States*

Kenneth M. Nicholas − *Department of Chemistry and Biochemistry, University of Oklahoma, Norman, Oklahoma 73019-5251, United States;* orcid.org/0000-0002-5180-1671

Complete contact information is available at: https://pubs.acs.org/10.1021/acscatal.3c05040

Author Contributions

‡B.G., A.C.H., and R.M. contributed equally to this work. The manuscript was written through the contributions of all authors. All authors have approved the final version of the manuscript.

Funding

National Science Foundation (NSF) CHE-1753187 and the Oklahoma Center for the Advancement of Science and Technology (OCAST) HR20-078.

Notes

The authors declare no competing financial interest.

■ ACKNOWLEDGMENTS

This work was supported by the NSF CHE-1753187 and the Oklahoma Center for the Advancement of Science and Technology (OCAST HR20-078). We thank Dr. Novruz Akhmedov, Dr. Steven Foster, and Dr. Douglas R. Powell from the Research Support Services, University of Oklahoma, for NMR, mass spectral, and X-ray crystallographic analysis, respectively. We want to thank Anae Bain and Ginny Kim for their helpful discussions. We also acknowledge support from the OU Supercomputing Center for Education & Research (OSCER).

■ REFERENCES

(1) (a) Bolm, C. A new iron age. *Nat. Chem.* **2009**, *1*, 420−420. (b) Bauer, E. B. Iron Catalysis: Historic Overview and Current Trends. In *Iron Catalysis II*, Bauer, E., Ed.; Springer International Publishing, 2015; pp. 1−18.

(2) Enthaler, S.; Junge, K.; Beller, M. Sustainable Metal Catalysis with Iron: From Rust to a Rising Star? *Angew. Chem., Int. Ed.* **2008**, *47*, 3317−3321.

(3) (a) Bolm, C.; Legros, J.; Le Paih, J.; Zani, L. Iron-Catalyzed Reactions in Organic Synthesis. *Chem. Rev.* **2004**, *104*, 6217−6254. (b) Front Matter. In *Iron Catalysis in Organic Chemistry*, 2008; pp I−XV. (c) Sherry, B. D.; Fürstner, A. The Promise and Challenge of Iron-Catalyzed Cross Coupling. *Acc. Chem. Res.* **2008**, *41*, 1500−1511. (d) Carreras, V.; Tanbouza, N.; Ollevier, T. The power of iron catalysis in diazo chemistry. *Synthesis* **2021**, *53*, 79−94.

(4) (a) Muthusamy, S.; Krishnamurthi, J. Heterocycles by Cycloadditions of Carbonyl Ylides Generated from Diazo Ketones. In *Synthesis of Heterocycles via Cycloadditions I*; Hassner, A., Ed.;

Springer: Berlin Heidelberg, 2008; pp 147−192. (b) Nicolaou, K. C.; Chen, J. S. The art of total synthesis through cascade reactions. *Chem. Soc. Rev.* **2009**, *38*, 2993−3009. (c) Padwa, A. A Chemistry Cascade: From Physical Organic Studies of Alkoxy Radicals to Alkaloid Synthesis. *J. Org. Chem.* **2009**, *74*, 6421−6441. (d) Vilotijevic, I.; Jamison, T. F. Epoxide-Opening Cascades in the Synthesis of Polycyclic Polyether Natural Products. *Angew. Chem., Int. Ed.* **2009**, *48*, 5250−5281. (e) Jones, A. C.; May, J. A.; Sarpong, R.; Stoltz, B. M. Toward a Symphony of Reactivity: Cascades Involving Catalysis and Sigmatropic Rearrangements. *Angew. Chem., Int. Ed.* **2014**, *53*, 2556−2591. (f) Ardkhean, R.; Caputo, D. F. J.; Morrow, S. M.; Shi, H.; Xiong, Y.; Anderson, E. A. Cascade polycyclizations in natural product synthesis. *Chem. Soc. Rev.* **2016**, *45*, 1557−1569.

(5) Nicolaou, K. C.; Edmonds, D. J.; Bulger, P. G. Cascade Reactions in Total Synthesis. *Angew. Chem., Int. Ed.* **2006**, *45*, 7134−7186.

(6) (a) Hunter, A. C.; Schlitzer, S. C.; Sharma, I. Synergistic Diazo-OH Insertion/Conia-Ene Cascade Catalysis for the Stereoselective Synthesis of γ-Butyrolactones and Tetrahydrofurans. *Chem.—Eur. J.* **2016**, *22*, 16062−16065. (b) Chinthapally, K.; Massaro, N. P.; Sharma, I. Rhodium Carbenoid Initiated O−H Insertion/Aldol/Oxy-Cope Cascade for the Stereoselective Synthesis of Functionalized Oxacycles. *Org. Lett.* **2016**, *18*, 6340−6343. (c) Massaro, N. P.; Stevens, J. C.; Chatterji, A.; Sharma, I. Stereoselective Synthesis of Diverse Lactones through a Cascade Reaction of Rhodium Carbenoids with Ketoacids. *Org. Lett.* **2018**, *20*, 7585−7589. (d) Hunter, A. C.; Chinthapally, K.; Bain, A. I.; Stevens, J. C.; Sharma, I. Rhodium/Gold Dual Catalysis in Carbene sp2 C−H Functionalization/Conia-ene Cascade for the Stereoselective Synthesis of Diverse Spirocarbocycles. *Adv. Synth. Catal.* **2019**, *361*, 2951−2958.

(7) (a) Soam, P.; Kamboj, P.; Tyagi, V. Rhodium-Catalyzed Cascade Reactions using Diazo Compounds as a Carbene Precursor to Construct Diverse Heterocycles. *Asian J. Org. Chem.* **2022**, *11*, No. e202100570. (b) England, D. B.; Eagan, J. M.; Merey, G.; Anac, O.; Padwa, A. The rhodium(II) carbenoid cyclization−cycloaddition cascade of α-diazo dihydroindolinones for the synthesis of novel azapolycyclic ring systems. *Tetrahedron* **2008**, *64*, 988−1001.

(8) (a) Padwa, A.; Austin, D. J. Ligand Effects on the Chemoselectivity of Transition Metal Catalyzed Reactions of α-Diazo Carbonyl Compounds. *Angew. Chem., Int. Ed.* **1994**, *33*, 1797−1815. (b) Masse, C. E.; Panek, J. S. Diastereoselective Reactions of chiral allyl and allenyl silanes with activated C: X. pi.-Bonds. *Chem. rev.* **1995**, *95*, 1293−1316. (c) Fleming, I.; Barbero, A.; Walter, D. Stereochemical control in organic synthesis using silicon-containing compounds. *Chem. Rev.* **1997**, *97*, 2063−2192. (d) Doyle, M. P.; Forbes, D. C. Recent Advances in Asymmetric Catalytic Metal Carbene Transformations. *Chem. Rev.* **1998**, *98*, 911−936. (e) Davies, H. M.; Nikolai, J. Catalytic and enantioselective allylic C−H activation with donor−acceptor-substituted carbenoids. *Org. Biomol. Chem.* **2005**, *3*, 4176−4187. (f) Moody, C. J. Enantioselective Insertion of Metal Carbenes into N-H Bonds: A Potentially Versatile Route to Chiral Amine Derivatives. *Angew. Chem., Int. Ed.* **2007**, *46*, 9148−9150. (g) Zhang, Z.; Wang, J. Recent studies on the reactions of α-diazocarbonyl compounds. *Tetrahedron* **2008**, *64*, 6577−6605. (h) Davies, H. M.; Denton, J. R. Application of donor/acceptor-carbenoids to the synthesis of natural products. *Chem. Soc. Rev.* **2009**, *38*, 3061−3071. (i) Doyle, M. P.; Duffy, R.; Ratnikov, M.; Zhou, L. Catalytic carbene insertion into C− H bonds. *Chem. Rev.* **2010**, *110*, 704−724. (j) Davies, H. M.; Morton, D. Guiding principles for site selective and stereoselective intermolecular C−H functionalization by donor/acceptor rhodium carbenes. *Chem. Soc. Rev.* **2011**, *40*, 1857−1869. (k) Zhu, S.-F.; Zhou, Q.-L. Transition-metal-catalyzed enantioselective heteroatom−hydrogen bond insertion reactions. *Acc. Chem. Res.* **2012**, *45*, 1365−1377. (l) Gillingham, D.; Fei, N. Catalytic X−H insertion reactions based on carbenoids. *Chem. Soc. Rev.* **2013**, *42*, 4918−4931. (m) Zheng, C.; You, S.-L. Recent development of direct asymmetric functionalization of inert C-H bonds. *RSC Adv.* **2014**, *4*, 6173−6214. (n) Ford, A.; Miel, H.; Ring, A.; Slattery, C. N.; Maguire, A. R.; McKervey, M. A. Modern organic synthesis with α-diazocarbonyl compounds. *Chem. Rev.* **2015**, *115*, 9981−10080. (o) Keipour, H.; Ollevier, T. Iron-Catalyzed Carbene Insertion Reactions of α-Diazoesters into Si−H Bonds. *Org. Lett.* **2017**, *19*, 5736−5739. (p) Boyarskikh, V.; Nyong, A.; Rainier, J. D. Highly diastereoselective sulfonium ylide rearrangements to quaternary substituted indolines. *Angew. Chem., Int. Ed.* **2008**, *47*, 5374−5377.

(9) Ou, C.; Ghosh, B.; Sharma, I. A Non-Diazo Approach to Functionalized (2-Furyl)-2-pyrrolidines through a Cascade Reaction of Enynal-Derived Zinc Carbenoids with β-Arylaminoketones. *Org. Chem. Front.* **2023**, *10*, 5933−5939.

(10) Zhu, S.-F.; Zhou, Q.-L. Iron-catalyzed transformations of diazo compounds. *Natl. Sci. Rev.* **2014**, *1*, 580−603.

(11) (a) Zhu, S.-F.; Cai, Y.; Mao, H.-X.; Xie, J.-H.; Zhou, Q.-L. Enantioselective iron-catalysed O−H bond insertions. *Nat. Chem.* **2010**, *2*, 546−551. (b) Aviv, I.; Gross, Z. Iron porphyrins catalyze the synthesis of non-protected amino acid esters from ammonia and diazoacetates. *Chem. commun.* **2006**, 4477−4479. (c) Aviv, I.; Gross, Z. Iron corroles and porphyrins as very efficient and highly selective catalysts for the reactions of α-diazo esters with amines. *Synlett* **2006**, *2006*, 951−953. (d) Aviv, I.; Gross, Z. Iron (III) Corroles and Porphyrins as Superior Catalysts for the Reactions of Diazoacetates with Nitrogen-or Sulfur-Containing Nucleophilic Substrates: Synthetic Uses and Mechanistic Insights. *Chem.—Eur. J.* **2008**, *14*, 3995−4005. (e) Mbuvi, H. M.; Woo, L. K. Catalytic C− H insertions using iron (III) porphyrin complexes. *Organometallics* **2008**, *27*, 637−645. (f) JaneáWang, Z. Cytochrome P450-catalyzed insertion of carbenoids into N−H bonds. *Chem. sci.* **2014**, *5*, 598−601. (g) Holzwarth, M. S.; Alt, I.; Plietker, B. Catalytic Activation of Diazo Compounds Using Electron-Rich, Defined Iron Complexes for Carbene-Transfer Reactions. *Angew. Chem., Int. Ed.* **2012**, *22*, 5351−5354. (h) Muthusamy, S.; Babu, S. A.; Gunanathan, C. Indium triflate: a mild and efficient Lewis acid catalyst for O−H insertion reactions of α-diazo ketones. *Tetrahedron lett.* **2002**, *43*, 3133−3136. (i) Yue, Y.; Wang, Y.; Hu, W. Regioselectivity in Lewis acids catalyzed X−H (O, S, N) insertions of methyl styryldiazoacetate with benzyl alcohol, benzyl thiol, and aniline. *Tetrahedron lett.* **2007**, *48*, 3975−3977. (j) Yoo, J.; Park, N.; Park, J. H.; Park, J. H.; Kang, S.; Lee, S. M.; Kim, H. J.; Jo, H.; Park, J.-G.; Son, S. U. Magnetically separable microporous Fe−porphyrin networks for catalytic carbene insertion into N−H bonds. *ACS Catal.* **2015**, *5*, 350−355. (k) Zhu, Y.; Liu, X.; Dong, S.; Zhou, Y.; Li, W.; Lin, L.; Feng, X. Asymmetric N-H Insertion of Secondary and Primary Anilines under the Catalysis of Palladium and Chiral Guanidine Derivatives. *Angew. Chem.* **2014**, *126*, 1662−1666. (l) Baumann, L. K.; Mbuvi, H. M.; Du, G.; Woo, L. K. Iron Porphyrin Catalyzed N−H Insertion Reactions with Ethyl Diazoacetate. *Organometallics* **2007**, *26*, 3995−4002.

(12) (a) Lee, W.-C. C.; Wang, D.-S.; Zhu, Y.; Zhang, X. P. Iron(III)-based metalloradical catalysis for asymmetric cyclopropanation via a stepwise radical mechanism. *Nat. Chem.* **2023**, *15*, 1569. (b) Gu, H.; Huang, S.; Lin, X. Iron-catalyzed asymmetric intramolecular cyclopropanation reactions using chiral tetramethyl-1,1′-spirobiindane-based bisoxazoline (TMSI-BOX) ligands. *Org. Biomol. Chem.* **2019**, *17*, 1154−1162. (c) Allouche, E. M. D.; Al-Saleh, A.; Charette, A. B. Iron-catalyzed synthesis of cyclopropanes by in situ generation and decomposition of electronically diversified diazo compounds. *Chem. commun.* **2018**, *54*, 13256−13259. (d) Morandi, B.; Dolva, A.; Carreira, E. M. Iron-Catalyzed Cyclopropanation with Glycine Ethyl Ester Hydrochloride in Water. *Org. Lett.* **2012**, *14*, 2162−2163.

(13) (a) Damiano, C.; Sonzini, P.; Gallo, E. Iron catalysts with *N*-ligands for carbene transfer of diazo reagents. *Chem. Soc. Rev.* **2020**, *49*, 4867−4905. (b) Griffin, J. R.; Wendell, C. I.; Garwin, J. A.; White, M. C. Catalytic C(sp3)−H Alkylation via an Iron Carbene Intermediate. *J. Am. Chem. Soc.* **2017**, *139*, 13624−13627. (c) Batista, V. F.; Pinto, G. A.; D, C.; Silva, A. M. S. Iron: A Worthy Contender in Metal Carbene Chemistry. *ACS Catal.* **2020**, *10*, 10096−10116. (d) Kaur, P.; Tyagi, V. Recent Advances in Iron-Catalyzed Chemical

https://doi.org/10.1021/acscatal.3c05040
ACS Catal. 2024, 14, 1292−1299

and Enzymatic Carbene-Transfer Reactions. *Adv. Synth. Catal.* **2021**, *363*, 877−905.
(14) (a) Faul, M. M.; Huff, B. E. Strategy and Methodology Development for the Total Synthesis of Polyether Ionophore Antibiotics. *Chem. Rev.* **2000**, *100*, 2407−2474. (b) Bermejo, A.; Figadère, B.; Zafra-Polo, M.-C.; Barrachina, I.; Estornell, E.; Cortes, D. Acetogenins from Annonaceae: recent progress in isolation, synthesis and mechanisms of action. *Nat. Prod. Rep.* **2005**, *22*, 269−303. (c) Saleem, M.; Kim, H. J.; Ali, M. S.; Lee, Y. S. An update on bioactive plant lignans. *Nat. Prod. Rep.* **2005**, *22*, 696−716. (d) Lorente, A.; Lamariano-Merketegi, J.; Albericio, F.; Álvarez, M. Tetrahydrofuran-Containing Macrolides: A Fascinating Gift from the Deep Sea. *Chem. Rev.* **2013**, *113*, 4567−4610.
(15) Hattori, M.; Hada, S.; Kawata, Y.; Tezuka, Y.; Kikuchi, T.; Namba, T. New 2, 5-Bis-aryl-3, 4-dimethyltetrahydrofuran Lignans from the Aril of *Myristica fragrans*. *Chem. Pharm. Bull.* **1987**, *35*, 3315−3322.
(16) Llopis, N.; Baeza, A. HFIP-Promoted Synthesis of Substituted Tetrahydrofurans by Reaction of Epoxides with Electron-Rich Alkenes. *Molecules* **2020**, *25*, 3464.
(17) Kobayashi, J.; Tsuda, M.; Ishibashi, M.; Shigemori, H.; Yamasu, T.; Hirota, H.; Sasaki, T. Amphidinolide F, a new cytotoxic macrolide from the marine dinoflagellate Amphidinium sp. *J. Antibiot. (Tokyo)* **1991**, *44*, 1259−1261.
(18) (a) Elliott, M. C. Saturated oxygen heterocycles. *J. Chem. Soc.* **2000**, 1291−1318. (b) Elliott, M. C.; Williams, E. Saturated oxygen heterocycles. *J. Chem. Soc.* **2001**, 2303−2340. (c) Wolfe, J. P.; Hay, M. B. Recent advances in the stereoselective synthesis of tetrahydrofurans. *Tetrahedron* **2007**, *63*, 261−290.
(19) (a) Nicolle, S. M.; Lewis, W.; Hayes, C. J.; Moody, C. J. Stereoselective Synthesis of Highly Substituted Tetrahydrofurans through Diverted Carbene O-H Insertion Reaction. *Angew. Chem., Int. Ed.* **2015**, *54*, 8485−8489. (b) Jing, C.; Xing, D.; Gao, L.; Li, J.; Hu, W. Divergent Synthesis of Multisubstituted Tetrahydrofurans and Pyrrolidines via Intramolecular Aldol-type Trapping of Onium Ylide Intermediates. *Chem.—Eur. J.* **2015**, *21*, 19202−19207.
(20) (a) Yang, J.-M.; Cai, Y.; Zhu, S.-F.; Zhou, Q.-L. Iron-catalyzed arylation of α-aryl-α-diazoesters. *Org. Biomol. Chem.* **2016**, *14*, 5516−5519. (b) Liu, B.; Zhu, S.-F.; Zhang, W.; Chen, C.; Zhou, Q.-L. Highly enantioselective insertion of carbenoids into N− H bonds catalyzed by copper complexes of chiral spiro bisoxazolines. *J. Am. Chem. Soc.* **2007**, *129*, 5834−5835.
(21) Babaahmadi, R.; Dasgupta, A.; Hyland, C. J. T.; Yates, B. F.; Melen, R. L.; Ariafard, A. Understanding the Influence of Donor-Acceptor Diazo Compounds on the Catalyst Efficiency of $B(C_6F_5)_3$ Towards Carbene Formation. *Chem.—Eur. J.* **2022**, *28*, No. e202104376.
(22) *CCDC 2285940 (3q), CCDC 2285941 (3i), CCDC2285942 (3u) contains the supplementary crystallographic data for this paper. These data can be obtained free of charge from the Cambridge Crystallographic Data Centre via* www.ccdc.cam.ac.uk/structures. Published (Date of access: December 18, 2023).
(23) Bull, J. A.; Croft, R. A.; Davis, O. A.; Doran, R.; Morgan, K. F. Oxetanes: Recent Advances in Synthesis, Reactivity, and Medicinal Chemistry. *Chem. Rev.* **2016**, *116*, 12150−12233.
(24) (a) Serafini, M.; Pirali, T.; Tron, G. C. Chapter Three - Click 1,2,3-triazoles in drug discovery and development: From the flask to the clinic? In *Adv. Heterocycl. Chem.*; Meanwell, N. A., Lolli, M. L., Eds.; Academic Press, 2021; Vol. *134*, pp 101−148. (b) Rani, A.; Singh, G.; Singh, A.; Maqbool, U.; Kaur, G.; Singh, J. CuAAC-ensembled 1,2,3-triazole-linked isosteres as pharmacophores in drug discovery: review. *RSC Adv.* **2020**, *10*, 5610−5635.
(25) See the supporting information page S60 for more details.

https://doi.org/10.1021/acscatal.3c05040
ACS Catal. 2024, 14, 1292−1299